Carboxymethyl chitosan hydrogel formulations enhance the healing process in experimental partial-thickness (second-degree) burn wound healing

Randys Caldeira Gonçalves[1] , Roberta Signini[2] , Luciana Martins Rosa[3] , Yuri Santana Pereira Dias[3] , Marina Clare Vinaud[4] , Ruy de Souza Lino Junior[4,*]

1. PhD. Universidade Federal de Goiás – Instituto de Patologia Tropical e Saúde Pública – Programa de Pós-Graduação em Medicina Tropical e Saúde Pública – Goiânia (GO), Brazil.
2. PhD. Universidade Estadual de Goiás – Campus de Ciências Exatas e Tecnológicas – Anápolis (GO), Brazil.
3. Graduate student. Universidade Federal de Goiás – Faculdade de Medicina – Goiânia (GO), Brazil.
4. PhD. Universidade Federal de Goiás – Instituto de Patologia Tropical e Saúde Pública – Departamento de Biociências e Tecnologia – Goiânia (GO), Brazil.

ABSTRACT

Purpose: This study aimed to elaborate a hydrogel constituted by carboxymethyl chitosan (CMC), hyaluronic acid (HA) and silver (Ag) and to evaluate its healing effect on partial-thickness burn wounds experimentally induced in rats. **Methods:** CMC was obtained by chitosan reacting with monochloroacetic acid. The carboxymethylation was confirmed by Fourier-transform infrared spectroscopy and hydrogen nuclear magnetic resonance (NMR). Scanning electron microscopy was used to determine the morphological characteristics of chitosan and CMC. After the experimental burn wound induction, the animals (n = 126) were treated with different CMC formulations, had their occlusive dressings changed daily and were followed through 7, 14 and 30 days. Morphometric, macroscopic and microscopic aspects and collagen quantification were evaluated. **Results:** Significative wound contraction, granulation tissue formation, inflammatory infiltration and collagen fibers deposit throughout different phases of the healing process were observed in the CMC hydrogels treated groups. **Conclusion:** The results showed that, in the initial phase of the healing process, the most adequate product was the CMC/HA/Ag association, while in the other phases the CMC/HA association was the best one to promote the healing of burn wounds.

Key words: Hydrogels. Carboxymethyl Chitosan. Experimental Burn Wound. Rats. General Pathologic Processes.

Introduction

Burn wounds are tissue injuries that may present partial or total destruction of the external covering tissue of the body. It may reach deep tissues, such as subcutaneous, muscle, tendons and even bones[1]. The main causes of burn wounds are heat, electricity, radiation, friction or contact with chemical agents. Its severity is directly related to the depth of the injury and it is classified as superficial-thickness burn wound (first degree), partial-thickness burn wound (second degree) and full-thickness burn wound (third degree)[1,2].

Such injuries are considered a severe public health issue[1,3] and the World Health Organization (WHO) estimates that about 24 million people suffer burn wounds each year around the world, most of them in low- and medium-income countries[4]. In Brazil, it is estimated that about a million people are victims of some kind of thermic trauma each year and 2,500 die directly or indirectly due to these injuries[5].

An ideal dressing for a burn wound should act directly on the site of the injury, stimulating the healing process. The dressings should have biological properties in order to ensure a high humidity environment, absorb exudates and toxic components from the wound, allow gas exchange and avoid bacterial contamination[6]. Besides, the dressing should not be toxic nor allergenic and should be composed by biocompatible materials[7,8].

Hydrogels are innovative biomaterials used in injuries dressings. Their tridimensional structure acts as a barrier against microorganisms, facilitates adhesion and cell proliferation, and its permeability enables the gas exchange necessary for tissue respiration[9,10]. Furthermore, hydrogels are easily rinsed, they remove the exudate and create a humid environment on the injury interface[11–14].

There are several types of dressings used in the burn wounds treatment, such as polymeric hydrogels and silver (Ag) incorporated dressings. Hydrogels may present different formulations, for instance, using chitosan (linear polymer of N-acetyl-D-glucosamine and a deacetylated glucosamine); diverse materials, which result in structural modifications; and hyaluronic acid ([HA] linear glycosaminoglycan composed by units of glucuronic acid and n-acetylglucosamine). The use of hydrogels as dressings in burn wounds has been recommended due to their essential characteristic of biological dressings, such as hydrophilicity, biodegradability, nonimmunogenic nature and healing properties[15–17].

Carboxymethyl chitosan (CMC) is a carboxymethylated derivative of the chitosan polymer, which presents higher biocompatibility and solubility in water than chitosan[18], and better antimicrobial performance[19]. While the HA presents several biological activities, such as elasticity of the intercellular tissue, fibrogenesis, angiogenic effect, anti-inflammatory and immunosuppressive characteristics[20]. Silver dressings are widely used in the treatment of burn wounds because they improve re-epithelialization, reduce levels of pain and decrease bacterial infections[21]. In spite of the use of nanoparticles and Ag salts being controversial due to its apparent toxicity, it has been shown that, when the polymeric hydrogels are associated to nanoparticles and Ag salts, the cutaneous toxicity is absent as there is a gradual liberation within the tissue[7,22].

The association of Ag and chitosan hydrogel induces a significant contraction of the wound, resulting in a quicker healing process. Also, the association of Ag with HA aids in the repair and regeneration of the injury[15,23–25]. On the other hand, the combination of chitosan and HA induced greater re-epithelialization of the wound[14,26,27]. Therefore, it is believed that the production of hydrogels of CMC incorporated with HA and Ag would result in a promising dressing with bioactive properties and increased efficacy regarding the healing of the wound.

This study aimed to evaluate the healing process of experimentally induced burn wounds in rats treated with CMC hydrogel incorporated with HA and Ag.

Methods

Carboxymethyl chitosan synthesis

Carboxymethyl chitosan was synthesized via heterogeneous carboxymethylation reaction based on the method described by Liu et al.[28]. Briefly, 10 g of chitosan in 220 mL of isopropanol were added under mechanical stirring (600 rpm) for 15 min. Soon after, 68 g of sodium hydroxide solution (50%) were added. This mixture was stirred for 1 h at room temperature. A solution of monochloroacetic acid (15 g) in isopropanol (20 mL) was then dripped onto the previously prepared mixture and the reaction was maintained for 24 h under constant stirring and at room temperature.

The mixture formed was filtered, washed with 70% ethanol. The synthesized CMC was suspended in 500 mL of methanol (80%) and left under constant stirring for 30 min. The suspension was neutralized with glacial acetic acid until neutral pH. Soon after, the suspension was filtered again and the obtained product was washed with absolute ethanol and dried at room temperature until constant weight.

Hydrogen nuclear magnetic resonance analysis (¹H NMR)

High resolution hydrogen NMR spectroscopy was used to characterize the original chitosan and the synthesized CMC. The spectrum was obtained at the NMR laboratory of the Chemistry Institute of the Universidade Federal de Goiás. Approximately 10 mg of the sample (chitosan and CMC) were added to 1.0 mL of D_2O/HCl mixture (1% v/v) and left under constant stirring for 24 h, resulting in a clear, viscous solution.

The ¹H NMR spectra were acquired on a Bruker spectrometer operating at 500 MHz at 80 °C. The interval between pulses was 3 seconds, 32 scans and the relaxation time was 7 seconds. Chemical shifts (δ) were expressed in dimensionless values (ppm) in relation to an internal tetramethylsilane (TMS) standard[29]. The visualization of the spectra was performed using the ACD LABS 12.0 software. The determination of the average degree of substitution (% GS) was carried out using the following Eqs. 1–4[30]:

$$f_6 = \left(\frac{1}{2}\right)\frac{A_a - A_b}{A_{H_2}} \tag{1}$$

$$f_3 = \frac{A_b}{A_{H_2}} \tag{2}$$

$$f_2 = \left(\frac{1}{2}\right)\frac{A_c}{A_{H_2}} \tag{3}$$

$$F = f_6 + f_3 + f_2 \tag{4}$$

where: A_a = area of the two hydrogens of the carboxymethyl group linked to C-6 and one hydrogen of the carboxymethyl group linked to C-3; A_b = area of a hydrogen of the carboxymethyl group linked to C-3; A_c = area of the two hydrogens of the carboxymethyl group linked to N linked to C-2; and A_{H_2} = area of hydrogen bonded to C-2 carbon.

The values obtained in f_6, f_3 and f_2 correspond to the carboxymethylation fractions at positions 6-O-, 3-O- and 2-N-, respectively, and F is the total fraction of carboxymethylation[30].

Infrared spectroscopy analysis

Infrared analyses were performed on KBr tablets using the spectrum Frontier full time infrared / near infrared (FTIR/NIR) spectrometer PerkinElmer (Perkin-Elmer Corp., Norwalk, CT) (Laboratório de Análise Instrumental do Campus de Anápolis de Ciências Exatas e Tecnológicas Henrique Santillo da Universidade Estadual de Goiás [CCET-UEG]), in order to observe the absorption bands characteristic of the original chitosan and the synthesized CMC. The FTIR spectral analysis[31] was performed within the range of wave numbers from 400 to 4000 cm⁻¹, with a resolution of 4 cm⁻¹.

Hydrogel formulations

Four different hydrogel formulations were prepared: (i) CMC, (ii) CMC and HA, (iii) CMC and Ag, (iv) CMC, HA and Ag). The hydrogels presented the following constant concentrations: CMC 2%, HA 0.2%, Ag nitrate 1% in sterile deionized water. The hydrogels were prepared inside a flow chamber in aseptic conditions in 1.5 mL sterile centrifuge tubes (Eppendorf), and were stored at –8 °C. The hydrogels formation was confirmed visually through the inverted flask method[25].

Scanning electron microscopy (SEM) analysis

A Jeol scanning electron microscope, JSM-6610, equipped with EDS, Thermo scientific NSS Spectral Imaging (Laboratório Multiusuário de Microscopia de Alta Resolução, Instituto de Física, UFG) was used to observe the morphology of the original chitosan, of the CMC synthesized and lyophilized hydrogel. The samples were fixed on an aluminum plate with the aid of double-sided graphite adhesive tape, covered by a thin layer of gold approximately 20 nm thick.

Thermogravimetric analysis

The thermal profiles of samples of the synthesized CMC and the hydrogels previously lyophilized were performed in the instrumental analysis laboratory of CCET/UEG, Anápolis, GO, Brazil. Approximately 30 mg of each sample was submitted to a temperature range of 25 to 800 °C, using a heating rate of 10 °C·min⁻¹, under a dynamic nitrogen atmosphere, with gas flow in the order of 20 mL·min⁻¹.

Burn wound healing studies

This study was approved by the Ethics Committee in Animal Use of the Universidade Federal de Goiás, protocol number 118/17.

A total of 126 Wistar (*Rattus norvegicus albinus*) rats 60 days old with a medium weight of 150 to 200 g were used. The animals were maintained in cages with free access to water and ration, with controlled temperature (24 ± 1 °C) with a light/dark cycle of 12 h. The animals were divided into 7 subgroups containing 18 animals each, according

to the treatment received, as follows: 1) PS – physiologic solution (NaCl 0.9%); 2) SS – 1% silver sulfadiazine (Prati-Donaduzzi, Brazil, batch 16A273), 3) Hy – 0.2% Hyaludermin (Systagenix, United Kingdom, batch 16804) commercial HA ointment; 4) CMC hydrogel, 5) CMC/HA hydrogel, 6) CMC/Ag hydrogel, 7) CMC/HA/Ag hydrogel. Groups 1, 2 and 3 were considered control groups, while groups 4 to 7 were the ones treated with hydrogel formulations and, therefore, considered the test groups. The animals were followed through 3 experimental days, 7, 14 and 30 days. At each experimental day, six animals from each group were euthanized.

Burn wound induction, dressings and euthanasia

On day zero, the animals were weighted, anesthetized through intraperitoneal administration of 0.1mL/100 g of animal weigh of ketamine 10% (União Química Farmacêutica Nacional S/A, Brazil), xylazine 2% (Sespo Indústria e Comércio Ltda, Brazil) and injection water. After the anesthesia, the dorsal region of the animal was prepared with trichotomy and antisepsis with 70% alcohol. The burn wound injuries were induced by scalding at 96 °C. The animals were gently maneuvered inside a polyvinyl chloride cylindric tube with a 2×2 cm^2 opening and sealed extremities[32–34].

The animals received daily occlusive sterile dressings hydrated with physiologic solution. The injuries were protected with physiologic solution humidified sterile gauze and cotton cloth. The specific topic agent of each treatment group was applied in a uniform layer sufficient to cover all the wound bed. The crusts on the wound bed were removed before the appliance of the dressings using tweezers and humidified gauze in order to prevent difficulty in the appliance of the product and its contact to the injury bed.

After the induction of the burn wound three animals were maintained per cage until the euthanasia day 7, 14 and 30, which was performed using a CO_2 chamber. The animals submitted to the burn wound induction were followed in order to detect pain and/or suffering by a veterinarian physician and received analgesic treatment during the first seven days with tramadol hydrochloride (Grünenthal Brasil Farmacêutica Ltda) diluted in the drinking water and with a daily intraperitoneal injection of tramadol, dosage of 12.5 mg/kg of body weight.

Morphometric evaluation of the wound contraction

The dimensions of the wound were measured with a ruler and photographed at day zero (burn wound induction day) and at days 14 and 30. The following formula was used to calculate the percentage of wound contraction (Eq. 5):

$$CD = \left[\frac{(Area\ D^0 - Area\ D^{Euthanasia})}{Area\ D^0} \right] \times 100 \qquad (5)$$

CD = contraction degree; D0 = day of burn wound induction; D Euthanasia = Days 14 and 30 after the injury induction.

The delimitation of the burn wound area was performed through the Image J software.

Macroscopic evaluation

At experimental days 7, 14 and 30 after the burn wound induction, the phases of the healing process (inflammatory, proliferative and remodeling) were macroscopically analyzed. The following parameters were evaluated: necrosis/crust, granulation tissue and re-epithelialization. The analysis of the pathologic processes was qualitative, as follows: absent (score 0), discrete (up to 25% of tissue commitment, score 1); moderate (between 26 and 50% of tissue commitment, score 2) and accentuated (more than 50% of tissue commitment, score 3)[32–34].

Microscopic evaluation

The microscopic evaluation was performed in fragments of the wound removed after the euthanasia and fixed in 10% buffered formaldehyde (pH 7.2) for 48 h, posteriorly included in paraffin, submitted to 4 µ transversal cuts using a microtome (Leica RM2255). The slides were stained by hematoxylin and eosin (H&E) and by picrosirius red (PS).

In the H&E-stained slides, the pathologic processes evaluated were polymorphonuclear cells inflammatory infiltration, mononuclear cells inflammatory infiltration and angiogenesis throughout the whole extension of the slide. These parameters were identified in a semi-quantitative form, as follows: absent (score 0), discrete (up to 25% of slide commitment, score 1), moderate (from 26 to 50% of slide commitment, score 2), accentuated (more than 50% of slide commitment, score 3).

The collagen quantification was performed in the PS-stained slides under polarized light. The analysis was performed using the Image J software (National Institutes of Health, EUA).

Statistical analysis

All statistical analysis was performed using the Sigma Stat 2.3 software. All variables were tested in order to

determine the normal distribution. The ones which presented normal distribution were analyzed through parametric tests, while the non-normal distribution variables were analyzed through nonparametric tests. In the morphometric analysis, according to the normal distribution and homogeneous variance, the analysis of variance (ANOVA) parametric test, followed by Tukey's post-test were used. In the macroscopic and microscopic analysis, according to the non-normal distribution, the nonparametric test Kruskal-Wallis followed by Dunn's post-test. All data are presented as mean and standard deviation or as median with maximum and minimum values. All analysis were considered significant when $p \leq 0.05$.

Results

Hydrogen nuclear magnetic resonance spectroscopy and infrared spectroscopy

The comparison of the chitosan spectra (Fig. 1a) with the CMC (Fig. 1b) suggests that in the carboxymethylation
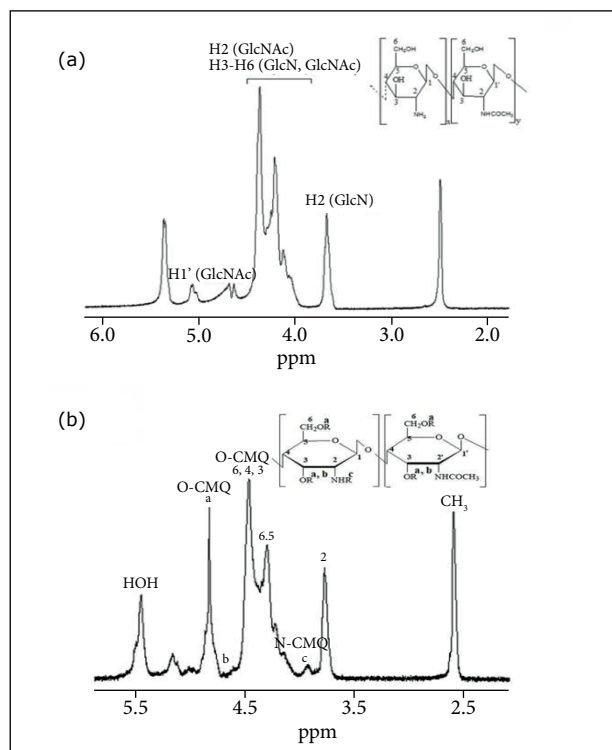

Figure 1 - Hydrogen nuclear magnetic resonance spectrum of (a) chitosan and (b) CMC. GlcNAc = N-acetylglucosamine and GlcN = glucosamine. The ^{1}H NMR spectra were determined using Bruker operating at 500 MHz at 80 °C, with a 3 s interval between pulses, 32 scans and a 7 s relaxation time. The visualization of the spectra was performed using the ACD LABS 12.0 software.

reaction the carboxymethyl groups (carboxylic acid) were effectively introduced into the polymeric matrix, proving the success of the synthesis. The ^{1}H NMR spectrum of chitosan exhibited a signal around 3.65 ppm related to the C2-linked hydrogen atom of the glucosamine ring (GlcN), a 2.5 ppm singlet characteristic of the methyl hydrogens of GlcNAc units (acetamide). The signals at 4.0 and 4.5 ppm are attributed to the hydrogen H3-H6 present in the GlcNA ring (glycopyranoside), while the signals occurring at 5.07 ppm are attributed to hydrogen bound to the anomeric carbon (C1) of the N-acetylglycosamine ring (H1) and the peak at 5.35 ppm is due to hydrogen bound to the anomeric carbon (C1) of the glycosamine ring (H1).

Figure 1b represents the ^{1}H NMR spectra of CMC, in which "a" corresponds to the two hydrogens of the carboxymethyl group attached to C (6) and the hydrogen of the carboxymethyl group attached to C (3) ($-CH_2COOD$ $4.6 < \delta < 4.9$ ppm), band "b" corresponds to the hydrogen of the carboxymethyl group linked to C (3) ($-CH_2COOD$ $4.5 < \delta < 4.6$ ppm). The "c" band corresponds to the two hydrogens of the carboxymethyl group linked to the nitrogen of the amino group (- + ND_2CH_2COOD $3.8 < \delta < 4.0$ ppm), showing N-carboxymethylation. However, N-carboxymethylation was very low, showing that the carboxymethylation occurred is predominant in the hydroxyl group.

From the analysis of the NMR-1 of the CMC and the Lamas equations (2008), the value obtained from the average degree of substitution in the carboxymethylation reaction, that is the number of carboxymethyl groups ($-CH_2COOH$) inserted in the polymer chain per monomer unit determined, was 1.42.

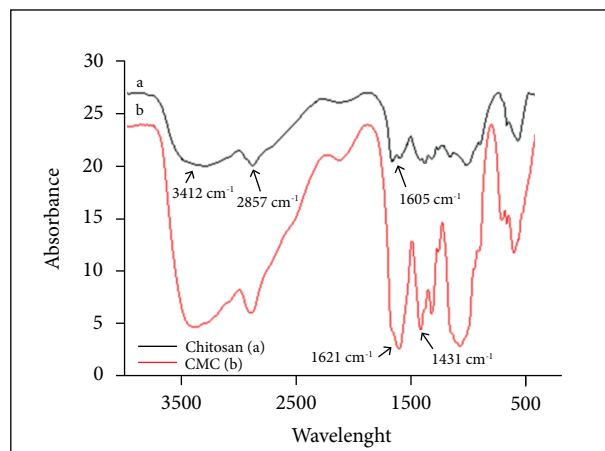The FTIR spectra of chitosan (Fig. 2a) showed an absorption band with a peak at 3412 cm^{-1} attributed

Figure 2 - Fourier-transform infrared spectroscopy of (**a**) chitosan (black line) and (**b**) CMC (red line).

to the stretching vibrations of the OH and NH bonds in the molecule. The absorption of the band at 1662 cm⁻¹ is attributed to the elongation of C = O of amides. The 1605 cm⁻¹ band results from the angular deformation of the NH bonds of the amino groups. There are also absorptions between 1643 and 2857 cm⁻¹, respectively, characteristics of the angular strain of the NH bonds of the amino groups and symmetric axial strain of the CH and CH2 groups. For CMC (Fig. 2b), an intense band at 1621 cm⁻¹ and a moderate band at 1431 cm⁻¹ were identified, due to the symmetry of –COOH asymmetric axial deformations, respectively, which confirms the introduction of the carboxymethyl groups.

Morphology of the lyophilized hydrogels

Chitosan and CMC had a continuous, irregular and rough surface (Fig. 3a–d). The surface of the lyophilized hydrogel of CMC (Fig. 3e and f) and CMC/HA (Fig. 3g and h) showed well-developed porosities and the hydrogel of CMC/Ag (Fig. 3i and j) and CMC/HA/Ag (Fig. 3k and l) had a surface with reliefs and a fibrous appearance under the polymeric matrix.
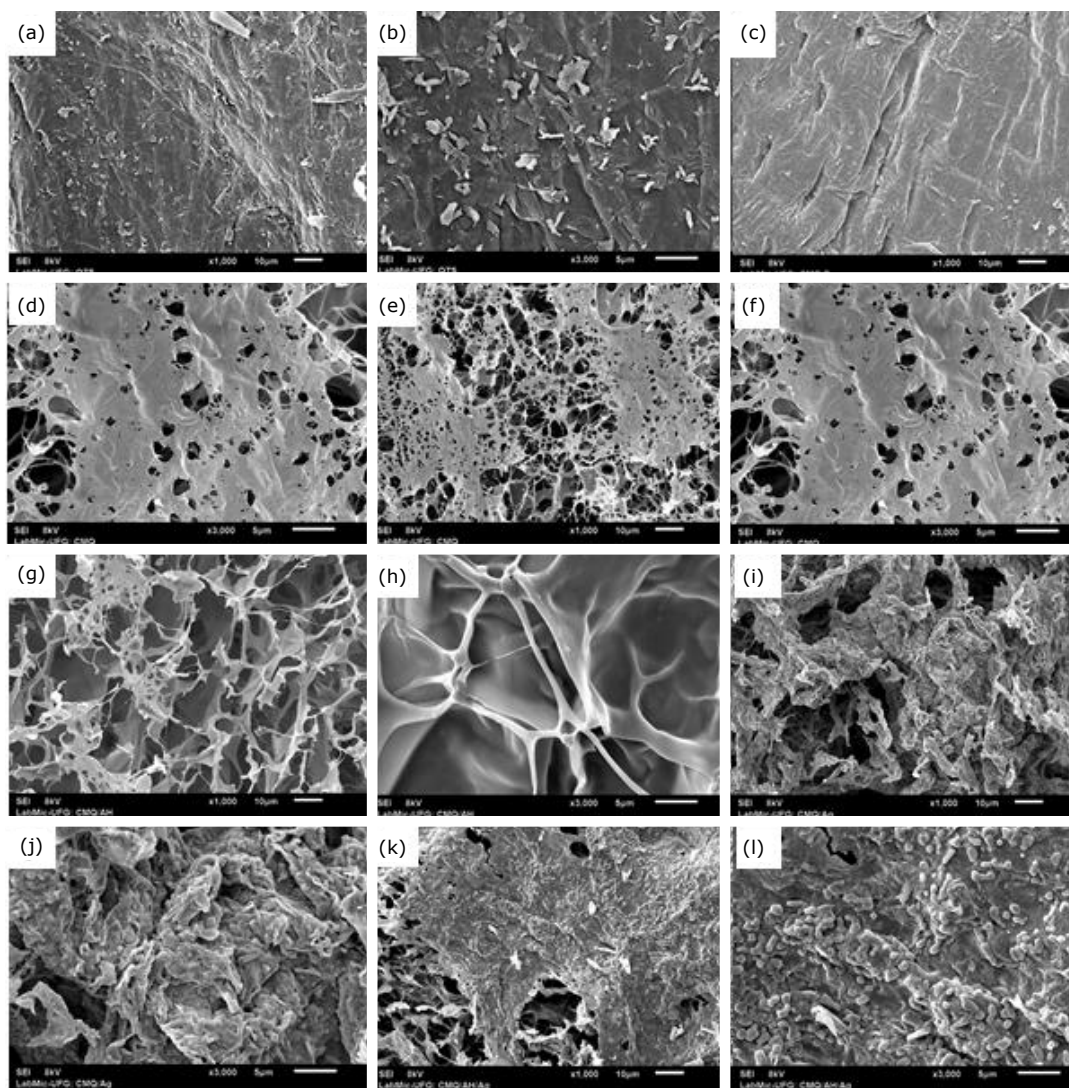

Figure 3 - Scan electron micrographs of the surfaces of the (**a**) original chitosan (scale 10 μm); (**b**) original chitosan (scale 5 μm); (**c**) synthetized CMC (scale 10 μm); (**d**) synthetized CMC (scale 5 μm); (**e**) CMC lyophilized hydrogel (scale 10 μm); (**f**) CMC lyophilized hydrogel (scale 5 μm); (**g**) CMC/HA lyophilized hydrogel (scale 10 μm); (**h**) CMC/HA lyophilized hydrogel (scale 5 μm); (**i**) CMC/Ag lyophilized hydrogel (scale 10 μm); (**j**) CMC/Ag lyophilized hydrogel (scale 10 μm); (**k**) CMC/HA/Ag lyophilized hydrogel (scale 10 μm); (**l**) CMC/HA/Ag lyophilized hydrogel (scale 5 μm).

Thermogravimetric analysis (TGA)

The TGA analysis showed three processes of mass loss, the first being related to dehydration (40 to 150 °C), followed by thermal degradation of the pyranose ring of the polymer chain (290 to 310 °C) and the decomposition of the carboxylic groups and glucosamine units of the polysaccharide structure (above 500 °C) (Fig. 4).
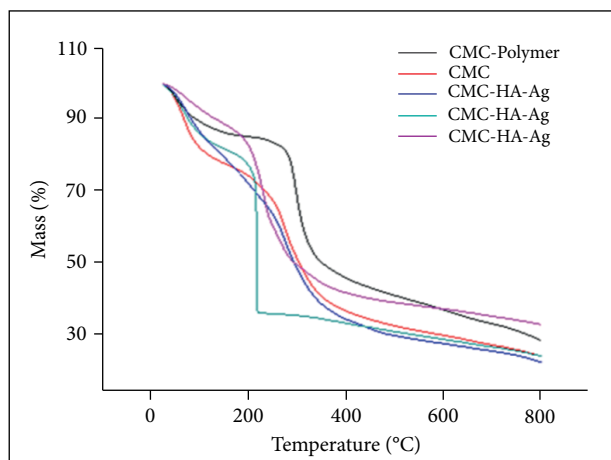

Figure 4 - Thermogravimetry curve of CMC and lyophilized hydrogels. CMC: carboxymethyl chitosan hydrogel; CMC/HA: carboxymethyl chitosan hydrogel and hyaluronic acid; CMC/Ag: carboxymethyl chitosan and silver hydrogel; CMC/HA/Ag: hydrogel of carboxymethyl chitosan, hyaluronic acid and silver.

Morphometric analysis

In the inflammatory phase, the groups treated with CMC, CMC/HA, CMC/Ag presented greater wound contraction than all the control groups. When comparing the hydrogel treatments, the CMC/HA/Ag presented lower wound contraction than the other treatments.

While in the proliferative phase, the groups treated with CMC, CMC/HA, CMC/Ag presented greater wound contraction than the PS control group. Regarding the hydrogel treatments, the CMC/HA/Ag presented lower wound contraction than the other treatments.

On the other hand, during the remodeling phase only the groups treated with CMC/HA and CMC/Ag presented greater wound contraction than the PS and SS control groups. Comparing the hydrogel treatments, the CMC treated group presented lower wound contraction than the CMC/HA treated one (Fig. 5).
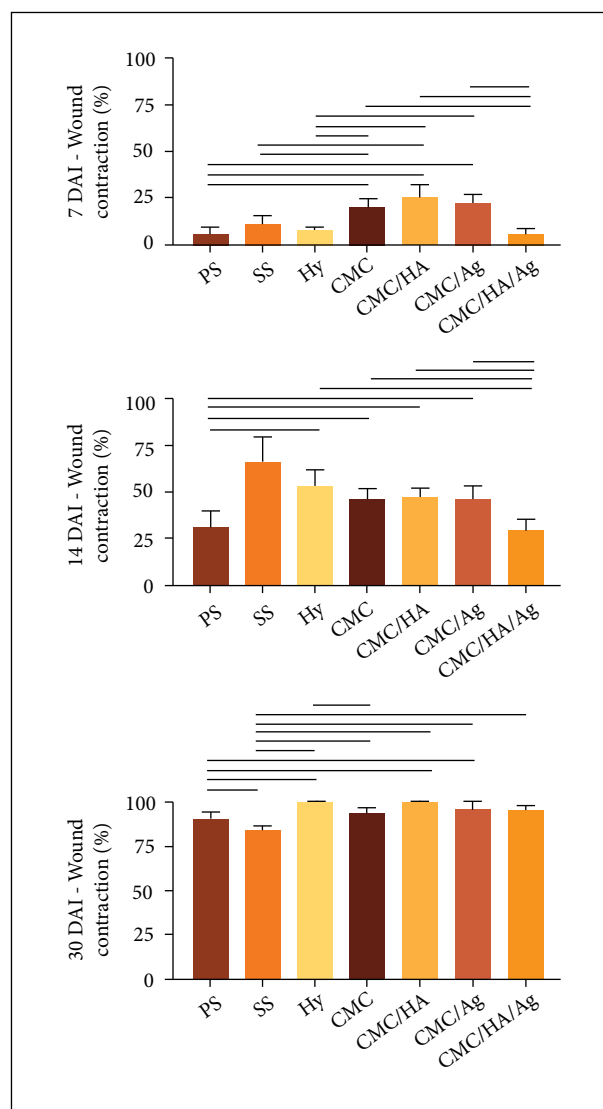

Figure 5 - Morphometric analysis of the contraction degree of partial-thickness burn wounds experimentally induced in Wistar rats. Results expressed in mean ± standard deviation of the percentage of contraction. n: number of animals. DAI: days after the injury induction. PS – physiologic solution (NaCl 0.9%); SS – 1% silver sulfadiazine; Hy – 0.2% Hyaludermin; CMC – carboxymethyl chitosan; CMC/HA – carboxymethyl chitosan and hyaluronic acid; CMC/Ag – carboxymethyl chitosan and silver; CMC/HA/Ag – carboxymethyl chitosan, hyaluronic acid and silver. Horizontal lines indicate the significant statistical difference. Statistical analysis: ANOVA and Tukey's post-test.

Macroscopic analysis

The macroscopic aspects of the healing process of partial-thickness burn wounds experimentally induced in

rats were compared regarding necrosis/crust, granulation tissue and re-epithelialization in the inflammatory (between 1st and 7th days), proliferative (between 7th and 14th days) and remodeling (between 14th and 30th days) phases of the healing process (Table 1).

In the inflammatory phase, the groups treated with CMC, CMC/HA and CMC/HA/Ag presented lower granulation tissue than the PS control group. Regarding the comparison between treatments, the CMC, CMC/HA and CMC/HA/Ag treated groups presented lower granulation tissue than the CMC/Ag treated one.

Table 1 - Macroscopic analysis of pathological processes in partial-thickness burn wounds experimentally induced in Wistar rats.

| | DAI | Control (n = 18) | | | Hydrogels (n = 18) | | | | p | Dunn's |
		PS	SS	Hy	CMC	CMC/HA	CMC/Ag	CMC/HA/Ag		
Necrosis/crust	7	3 (2–3)	0 (0–1)	3 (3–3)	3 (2–3)	3 (2–3)	2.5 (2–3)	3 (3–3)	< 0.001*	Hy > SS CMC/HA/Ag > SS PS > SS CMC/HA > SS CMC > SS CMC/Ag > SS
	14	2 (1–3)	1 (0–2)	0 (0–2)	0.5 (0–1)	0.5 (0–1)	1.5 (0–3)	0 (0–1)	0.027*	PS > CMC/HA/Ag PS > CMC/HA PS > CMC PS > Hy
	30	2 (2–3)	0 (0–1)	0 (0–0)	0 (0–1)	0 (0–0)	0 (0–1)	0 (0–0)	< 0.001*	PS > CMC/HA/Ag PS > CMC/HA PS > Hy PS > CMC/Ag PS > SS PS > CMC
Granulation tissue	7	2 (1–2)	0 (10–0)	0 (0–0)	0 (0–1)	0 (0–1)	1 (0–2)	0 (0–1)	< 0.001*	PS > Hy PS > SS PS > CMC/HA/Ag PS > CMC/HA PS > CMC CMC/Ag > Hy CMC/Ag > SS CMC/Ag > CMC/HA/Ag CMC/Ag > CMC/HA CMC/Ag > CMC
	14	2.5 (2–3)	1 (0–2)	3 (3–3)	3 (3–3)	3 (3–3)	2 (1–3)	3 (2–3)	> 0.001*	Hy > SS CMC > SS CMC/HA > SS CMC/HA/Ag > SS PS > SS
	30	0 (0–0)	1 (0–1)	0 (0–0)	0 (0–0)	0 (0–0)	0 (0–0)	0 (0–0)	> 0.001*	SS > CMC/HA/Ag SS > CMC/HA SS > CMC/Ag SS > CMC SS > Hy SS > PS
Re-epithelialization	7	0 (0–0)	0 (0–0)	0 (0–0)	0 (0–0)	0 (0–0)	0 (0–0)	0 (0–0)	1	
	14	0.5 (0–2)	0 (0–1)	1 (1–1)	1 (0–1)	1 (0–1)	0 (0–1)	1 (0–1)	0.126	
	30	3 (2–3)	3 (3–3)	3 (3–3)	3 (3–3)	3 (3–3)	3 (3–3)	3 (3–3)	0.022*	CMC > PS CMC/HA > PS CMC/Ag > PS CMC/HA/Ag > PS SS > PS Hy > PS

Results expressed in median (minimum – maximum). n: number of animals. DAI: days after the injury induction. PS: physiologic solution (NaCl 0.9%); SS: 1% silver sulfadiazine; Hy: 0.2% Hyaludermin; CMC: carboxymethyl chitosan; CMC/HA: carboxymethyl chitosan and hyaluronic acid; CMC/Ag: carboxymethyl chitosan and silver; CMC/HA/Ag: carboxymethyl chitosan, hyaluronic acid and silver. Statistical analysis: Kruskal Wallis and Dunn's post-test. * p < 0.05.

In the proliferative phase, the groups treated with CMC, CMC/HA and CMC/HA/Ag presented lower necrosis/crust than the PS control group.

While, in the remodeling phase, the groups treated with all the hydrogel formulations presented lower necrosis and greater re-epithelialization than the PS control group.

Microscopic analyses

The histopathologic analyses evaluated the intensity of the general pathologic processes during the inflammatory, proliferative and remodeling phases of the healing process, which are described in Table 2, and Figs. 6–8.

In the inflammatory phase was possible to observe that the groups treated with CMC/Ag and CMC/HA/Ag presented greater intensity of polymorphonuclear (PMN) cells infiltration in comparison to the PS and SS control groups.

During the proliferative phase, the hydrogel treatments did not interfere in the general pathologic processes analyzed.

While in the remodeling phase, the groups treated with CMC presented greater intensity of PMN cells infiltration than the PS and Hy control groups. The CMC treated group also presented greater intensity of PMN cells infiltration than the CMC/HA treated group. Regarding angiogenesis, it was greater in the CMC/Ag treated group than the PS and Hy control groups.

Regarding the quantitative analysis of collagen fibers during the inflammatory phase, all the hydrogel treatments induced greater collagen quantification than the PS and SS control groups. When comparing the hydrogel treatments, the group treated with CMC/HA presented more collagen than the other treatments. The group treated with CMC/HA/Ag presented greater collagen than the CMC/Ag (Fig. 9).

Table 2 - Microscopic analysis of the general pathologic processes related to the healing process of partial-thickness burn wounds experimentally induced in Wistar rats.

Pathologic processes	DAI	Control (n = 18)			Hydrogels (n = 18)				P	Dunn's
		PS	SS	Hy	CMC	CMC/HA	CMC/Ag	CMC/HA/Ag		
PMN infiltration	7	2 (1–3)	1 (1–2)	3 (3–3)	2 (1–3)	3 (2–3)	3 (3–3)	3 (3–3)	0.001	CMC/Ag > SS CMC/Ag > PS CMC/HA/Ag > SS CMC/HA/Ag > PS HY > SS HY > PS CMC/HA > SS
	14	1 (1–1)	2 (1–3)	1 (0–1)	1 (1–2)	1 (1–1)	1 (1–1)	2 (1–2)	0.005	SS > HY CMC/HA/Ag > Hy
	30	1 (1–0)	1 (0–1)	0 (0–0)	1 (1–2)	0 (0–0)	1 (0–2)	0 (0–1)	0.009	CMC > Hy CMC > CMC/HA CMC > PS
MN infiltration	7	2 (2–3)	3 (3–3)	2 (2–3)	2 (2–3)	2 (2–2)	3 (3–3)	2 (2–3)	0.002	SS > CMC/HA SS > CMC/HA/AG CMC/Ag > CMC/HA CMC/Ag > CMC/HA/Ag
	14	2 (2–3)	2 (2–2)	2 (1–2)	3 (2–30)	3 (2–3)	2 (2–3)	3 (2–3)	0.088	
	30	1 (1–2)	2 (1–2)	1 (1–1)	2 (1–2)	1 (0–1)	1 (1–2)	1 (1–2)	0.102	
Angiogenesis	7	3 (3–3)	3 (3–3)	3 (3–3)	3 (3–3)	3 (3–3)	3 (3–3)	3 (3–3)	1	
	14	3 (2–3)	2 (2–2)	3 (2–3)	3 (3–3)	3 (3–3)	3 (3–3)	3 (3–3)	0.001	CMC > SS CMC/HA > SS CMC/Ag > SS CMC/HA/Ag > SS PS > SS Hy > SS
	30	1 (1–1)	1 (1–2)	1 (1–1)	2 (1–2)	2 (2–2)	2 (1–3)	2 (1–3)	0.010	CMC/Ag > Hy CMC/Ag > PS

Results expressed in median (minimum – maximum). n: number of animals. DAI: days after the injury induction. PMN: polymorphonuclear cells; MN: mononuclear cells; PS: physiologic solution (NaCl 0.9%); SS: 1% silver sulfadiazine; Hy: 0.2% Hyaludermin; CMC: carboxymethyl chitosan; CMC/HA: carboxymethyl chitosan and hyaluronic acid; CMC/Ag: carboxymethyl chitosan and silver; CMC/HA/Ag: carboxymethyl chitosan, hyaluronic acid and silver. Statistical analysis: Kruskal Wallis and Dunn's post-test.
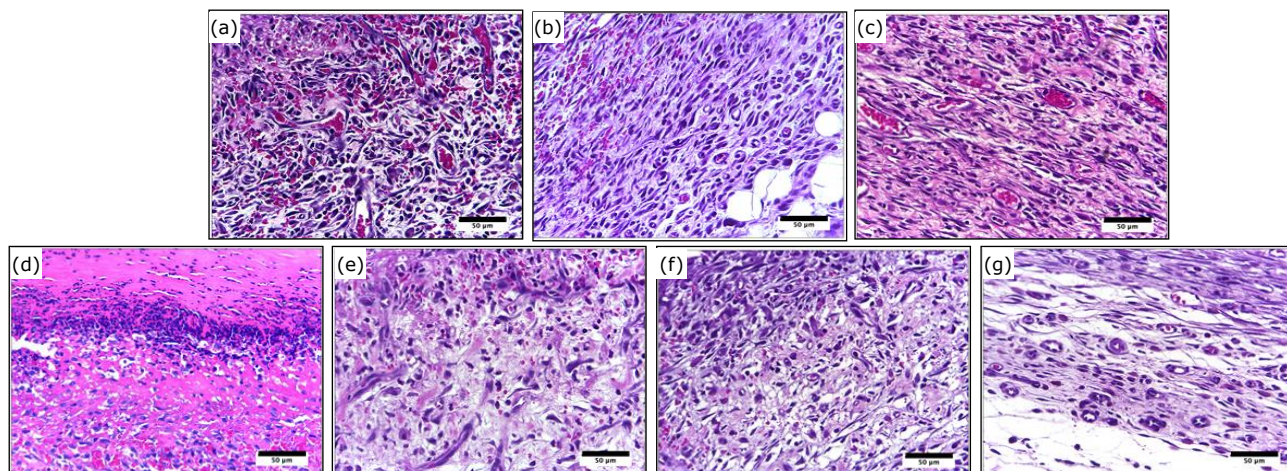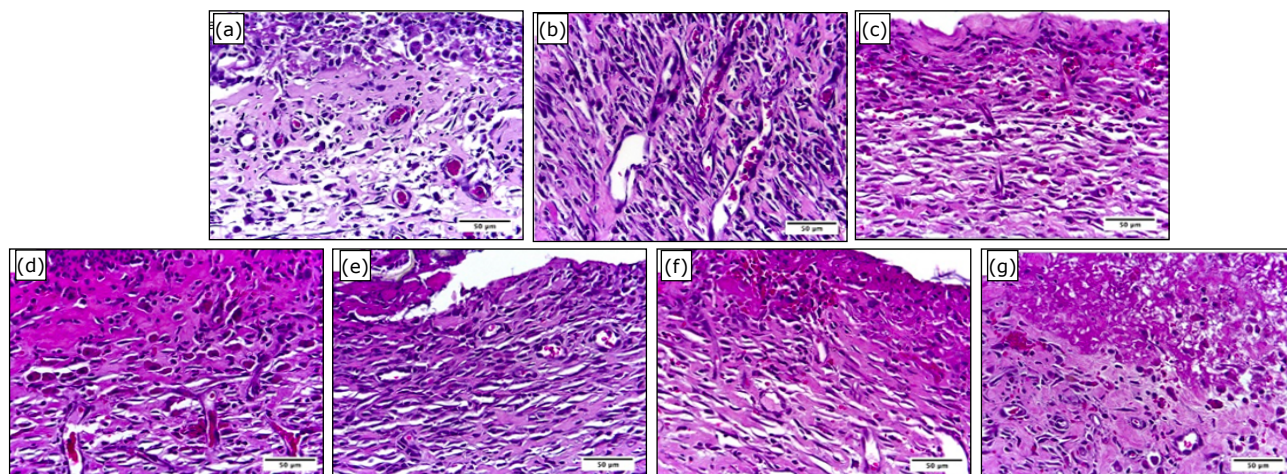
Figure 6 - Photomicrograph of partial-thickness burn wounds experimentally induced in Wistar rats 7 days after the injury induction. (**a**) Physiologic solution (NaCl 0.9%) treatment, (**b**) 1% SS treatment, (**c**) 0.2% Hy, (**d**) CMC hydrogel treatment, (**e**) CMC/HA hydrogel treatment, (**f**) CMC/Ag hydrogel treatment, (**g**) CMC/HA/Ag hydrogel treatment. Objective × 40. Scale in μm.

Figure 7 - Photomicrograph of partial-thickness burn wounds experimentally induced in Wistar rats 14 days after the injury induction. (**a**) Physiologic solution (NaCl 0.9%) treatment, (**b**) 1% SS treatment, (**c**) 0.2% Hy, (**d**) CMC hydrogel treatment, (**e**) CMC/HA hydrogel treatment, (**f**) CMC/Ag hydrogel treatment, (g) CMC/HA/Ag hydrogel treatment. Objective × 40. Scale in μm.
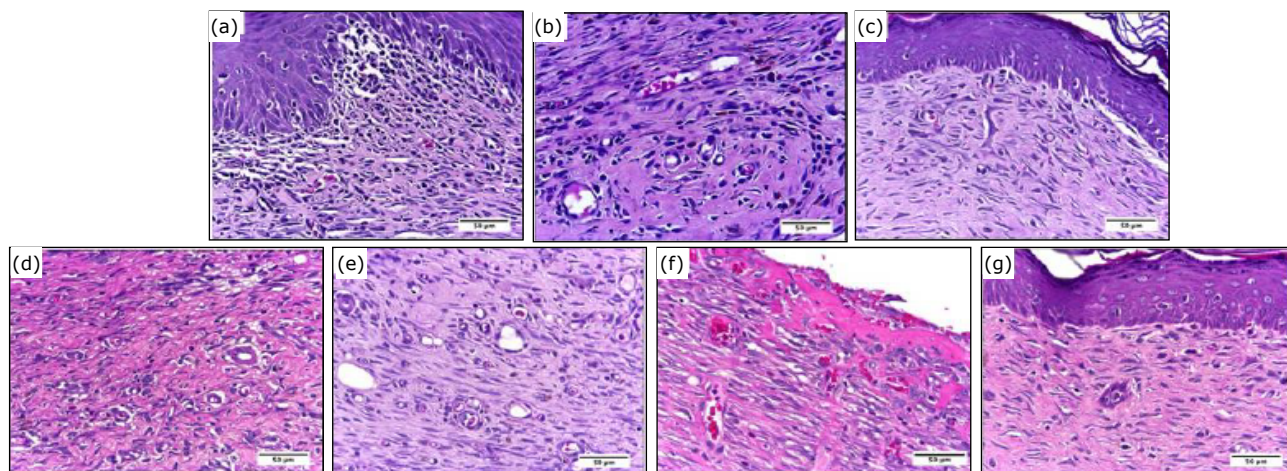

Figure 8 - Photomicrograph of partial-thickness burn wounds experimentally induced in Wistar rats 30 days after the injury induction. (**a**) Physiologic solution (NaCl 0.9%) treatment, (**b**) 1% SS treatment, (**c**) 0.2% Hy, (**d**) CMC hydrogel treatment, (**e**) CMC/HA hydrogel treatment, (**f**) CMC/Ag hydrogel treatment, (**g**) CMC/HA/Ag hydrogel treatment. Objective × 40. Scale in μm.
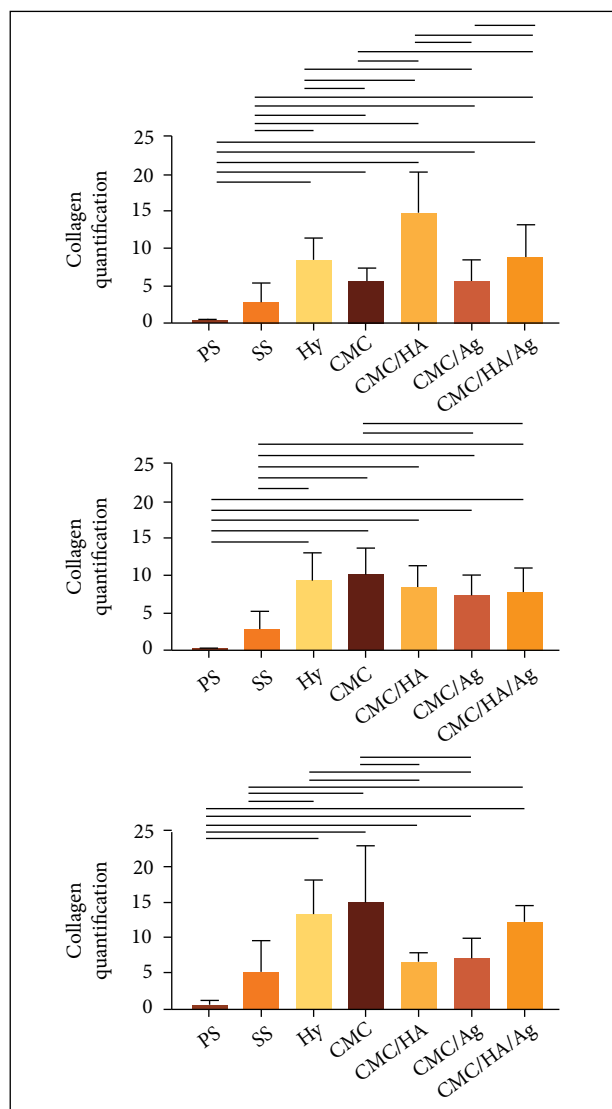
greater collagen deposition than the CMC/Ag and CMC/HA/Ag treated ones.

While in the remodeling phase, all the hydrogel treatments presented greater collagen deposition than the PS control group. The comparison between treatments showed that the CMC treated group presented more collagen deposition than CMC/HA and CMC/Ag treated ones.

Discussion

Chitosan can be easily carboxymethylated to improve its solubility, biodegradability and biocompatibility. Carboxymethylation is an etherification reaction that consists of replacing the hydrogens present in the amino and hydroxyl groups of the chitosan structure, with carboxymethyl groups (CH2COOH)[29,35]. In the present study, carboxymethylation reaction of chitosan was carried out with monochloroacetic acid in isopropanol alcohol in alkaline conditions through a 24 h reaction. Sodium hydroxide reacts with chitosan and promotes the protonation of amino groups (-NH2) and/or hydroxyl groups (-OH) arranged in the molecule[36], while monochloroacetic acid acts as a carboxymethylation agent, promoting reactions between chitosan groups to form CMC[37].

After the carboxymethylation reaction carried out in this study, the comparison of the ^{1}H NMR and FTIR spectra of chitosan and synthesized CMC confirmed that the chemical modifications of chitosan occurred successfully under the conditions used in this study. In the ^{1}H NMR spectra of CMC, the presence of signs of the hydrogens of the carboxymethyl group linked to C (6) and C (3) was observed in 4.6 and 4.9 ppm, respectively, confirming data reported in the literature[29,31]. The signs of the carboxymethyl group hydrogens linked to the nitrogen of the amino group were observed in the chemical displacement interval $3.8 < \delta < 4.0$ ppm, with the occurrence of N-carboxymethylation (carboxymethylation in amino groups) in low extension/ intensity[38].

In the FTIR spectra of CMC, the main changes were observed in the range of 1621 and 1431 cm^{-1}, attributed to the introduction of carboxylic groups in the polymer chain, similar to that described previously by other authors[19,29,39]. It has been reported that the carboxylic groups present in the CMC improve the hydrophilicity of the molecule, improving its use in the treatment of wounds[40,41].

Scanning electron microscopy revealed that chitosan and CMC had a continuous flat surface with roughness under the polymer matrix, the lyophilized hydrogel of CMC and CMC/HA a well-developed porous structure and lyophilized hydrogel of CMC/Ag and CMC/AH/Ag microstructure with reliefs and fibrous appearance under the polymeric matrix.

Figure 9 - Microscopic evaluation of collagen fibers deposition in partial-thickness burn wounds experimentally induced in Wistar rats. Results expressed in mean ± standard deviation. DAI: days after the injury induction. PS: physiologic solution (NaCl 0.9%); SS: 1% silver sulfadiazine, Hy: 0.2% Hyaludermin, CMC: carboxymethyl chitosan, CMC/HA: carboxymethyl chitosan and hyaluronic acid, CMC/Ag: carboxymethyl chitosan and silver, CMC/HA/Ag: carboxymethyl chitosan, hyaluronic acid and silver. Horizontal lines indicate the significant statistical difference. Statistical analysis: ANOVA and Tukey's post-test.

In the proliferative phase, all the hydrogel treatment groups presented greater collagen quantification than the PS and SS control groups. The comparison between the treatments showed that the CMC treated group presented

According to the literature, the porous surface of a dressing has great importance in the wound healing process, since it promotes a moist environment and oxygenation at the wound site and removes exudate[42].

The TGA results showed that CMC and lyophilized hydrogels have a thermal degradation profile in three stages of mass loss. The first stage refers to the evaporation of water physically adsorbed in the polymeric network[25] and started in the temperature range of 40 to 150 °C, with a mass loss of 3 to 14%. The second stage of mass loss, attributed to the beginning of thermal degradation of the pyranose ring of the polymeric chain[43], started at about 290 °C and extends to 310 °C with a mass loss ranging from 30 to 40%. The third stage occurs at temperatures above 500 °C, corresponding to the decomposition of the carboxylic groups and glucosamine units of the polysaccharide structure[44].

This study evaluated the healing process in partial-thickness burn wounds experimentally induced in Wistar rats after treatment with hydrogel formulations. The complex biological process of healing includes a wide range of macroscopic and microscopic parameters, such as necrosis/crust and granulation tissue formation, re-epithelialization, inflammatory cells infiltration, angiogenesis and collagen fibers deposition[45]. It has been shown that the composition of the dressing used on the care of different wounds are critical on the evolution of the healing process regarding several aspects, such as the ones evaluated in this study[46].

The benefits of the isolated application of hydrogels, CMC and HA in wound dressings for the treatment of several types of wounds has been described previously[15,17,20,23,26,35]. However, the association of such substances and their beneficial effects on the healing process of burn wounds experimentally induced in rats is being described for the first time in this study.

The dressings evaluated in this study showed easy handling and appliance during the experiment period of 30 days and there was no sign of infection in the treated injuries. It is important to highlight that both chitosan and CMC favor the chemotaxis of neutrophils, which prevents the wound infection[38,47–50]. It has been demonstrated that CMC presents enhance biological properties when compared to chitosan, such as increased solubility and biocompatibility, greater viscosity and moisture retention, and improved antimicrobial activity. These enhancements demonstrate why CMC is a better choice than chitosan for a wound dressing material[35].

During the inflammatory phase, the wound contraction was greater after the treatment with CMC hydrogel formulations. It was also possible to observe more granulation tissue, PMN inflammatory infiltration and collagen fibers deposition. The association of CMC with HA and Ag was the hydrogel formulation that mostly influenced these aspects at the initial days of the healing process.

Hydrogels are biomaterials with important healing properties, such as permeability to metabolites, nonirritant and nonreactive towards biological tissue. The high-water content of hydrogel formulations is important in the granulation tissue formation. Also, hydrogel has been considered suitable for all phases of the healing process[51]. Humidity has been described as an important factor regarding the collagen deposition, which is directly related to the contraction of the wound[52].

On the other hand, chitosan has been shown to present an important effect as PMN chemotactic, inducing the production of complement 5a (C5a), induction of interleukin-8 (IL-8) and collagen production by *in situ* fibroblasts, therefore activating inflammatory migration into the wounded area in experimental open wound in dogs[53]. These findings are in accordance to this study in which there is an increase in PMN inflammatory infiltration and collagen quantification after the chitosan hydrogels treatments.

Regarding the treatment of experimental burn wounds, chitosan has been shown to significantly induce a greater wound contraction and re-epithelialization of the injuries during the inflammatory phase, approximately up to 7 days after the injury induction[54]. Similar results to the ones found in this study. It has been reported important antimicrobial effect of chitosan alone and impregnated with Ag in the treatment of experimental burn wounds during the first days of the healing process[55].

The addition of HA to the hydrogel formulation has been shown to contribute to the humidity of the environment, since it is highly osmotic and hygroscopic. It is an important stimulator of the cell proliferation and migration[56]. These findings explain why the groups that presented HA in addition to CMC presented higher PMN inflammatory infiltration, granulation tissue and collagen deposition.

During the proliferative phase of the healing process, the hydrogel treatments induced greater wound contraction and collagen fibers deposition. It was also possible to observe less necrosis after the hydrogel treatments. The association of CMC with HA was the formulation that better influenced these aspects.

The addition of HA to the CMC formulation increased its effect on the healing process. It stimulates the proliferation and migration of epithelial cells, modulates inflammatory responses, increases angiogenesis and eliminates oxygen reactive species derived from inflammatory cells. It also increases the collagen fibers deposition in the wound site[13,57–61].

The efficacy of the association of chitosan, HA and arginine in promoting the healing process in experimental burn wounds in rats have been described previously[14,18]. As well as its different formulations, such as dextran-based hydrogels loaded with chitosan microparticles containing growth factor induced fastest healing burn wounds experimentally induced in rats[33].

While, during the remodeling phase, the hydrogel treatments induced greater wound contraction, re-epithelialization, angiogenesis and collagen fibers deposition with less necrosis. As observed in the proliferative phase, the association of CMC with HA was the formulation with best influence on these aspects.

Polymeric membranes containing chitosan, HA and arginine derivates have shown healing properties regarding experimentally induced burn wounds in rats, demonstrating the potential of such polymers as burn wound dressings. The use of such dressings increased the wound contraction[14], which is in accordance with the results of this research. Chitosan and HA have been shown to induce greater wound closure also in excisional wounds experimentally induced in rats, improving the healing process[25].

The CMC associated to HA treatments induced lower necrosis/crust formation than the traditional Ag-based treatment during the inflammatory, proliferative and remodeling phases of the healing process. Also, the granulation tissue formation and the re-epithelialization were induced by the CMC/HA treatment. As described previously, the appliance of a N-carboxymethyl chitosan membrane has significantly improved the healing rate of burn wounds experimentally induced in rats regarding the reduction in necrosis, increase in granulation tissue and re-epithelialization[62]. These results may be explained by the improved humidity, cytocompatibility and antibacterial activity of chitosan[63,64]. The enhanced re-epithelialization has been described in natural polymers alongside with the characteristics of hemostatic, antibacterial, anti-inflammatory and wound healing properties[12,58].

The increase in angiogenesis observed in the hydrogel treated groups during the remodeling phase is explained by the induction of vascular endothelial growth factor expression, as described in the study of the effect of carboxymethylcellulose sodium/sodium alginate/chitosan hydrogel in deep second-degree burn wounds[64]. Other important effects observed were the down regulation of basic fibroblast growth factor in the early periods of wound healing and up regulation at a later stage and decreased levels of tumor necrosis factor alpha (TNF-alpha) and interleukin-6 (IL-6)[64].

It has been demonstrated previously that N-carboxymethyl chitosan formulations induced reduction in wound size, accelerated wound healing and greater collagen deposition in deep second-degree burn wounds experimentally induced in rats[62], which is in accordance to the collagen quantification in these results. *In vitro* studies have demonstrated the chitosan capability of stimulating fibroblasts and keratinocytes, which are important cells in the healing process, especially in the collagen production[11,49,61].

■ Conclusions

The carboxymethylation reaction was carried out successfully and was efficient in the hydrogel production. The hydrogels consisting of CMC, HA and Ag nitrate in different formulations indicated good compatibility between the components and thermal stability. This study is the first description of the effect of CMC associated to HA and Ag on the healing process of partial-thickness burn wounds experimentally induced in rats. The CMC hydrogel treatments showed positive effects in some aspects of the healing process. It was possible to determine that, in the early phases of the healing process, during the inflammatory phase, the use of the association of CMC with HA and Ag is the best formulation in order to enhance several aspects of the healing process. While in the following phases of the healing process, proliferative and remodeling ones, the best formulation in order to enhance the healing process is CMC associated to HA.

■ Authors' contribution

■ Data availability statement

Data will be available upon request.

■ Funding

Acknowledgments

References

1. Jeschke MG, van Baar ME, Choudhry MA, Chung KK, Gibran NS, Logsetty S. Burn injury. Nat Rev Dis Primers. 2020;6:11. https://doi.org/10.1038/s41572-020-0145-5

2. Martin NA, Falder S. A review of the evidence for threshold of burn injury. Burns. 2017;43(8):1624–39. https://doi.org/10.1016/j.burns.2017.04.003

3. Lee SM, Park IK, Kim YS, Kim HJ, Moon H, Mueller S, Jeong Y-I. Physical, morphological, and wound healing properties of a polyurethane foam-film dressing. Biomater Res. 2016;20:37. https://doi.org/10.1186/s40824-016-0084-0

4. [WHO] World Health Organization. Violence and Injury Prevention: Burns. WHO. [cited 2021 Mar 14]. Available from: www.who.int/violence_injury_prevention/other_injury/burns/en/

5. Pan R, Silva MTR, Fidelis TLN, Vilela LS, Silveira-Monteiro CA, Nascimento LC. Conhecimento de profissionais de saúde acerca do atendimento inicial intra-hospitalar ao paciente vítima de queimaduras. Rev Gaúcha Enferm. 2018;39:e2017-0279. https://doi.org/10.1590/1983-1447.2018.2017-0279

6. Meng H, Chen L, Ye Z, Wang S, Zhao X. The effect of a self-assembling peptide nanofiber scaffold (peptide) when used as a wound dressing for the treatment of deep second degree burns in rats. J Biomed Mater Res B Appl Biomater. 2008;89B(2):379–91. https://doi.org/10.1002/jbm.b.31226

7. Bano I, Arshad M, Yasin T, Ghauri MA, Younus M. Chitosan: a potential biopolymer for wound management. Int J Biol Macromol. 2017;102:380–3. https://doi.org/10.1016/j.ijbiomac.2017.04.047

8. Sharma S, Swetha KL, Roy A. Chitosan-Chondroitin sulfate based polyelectrolyte complex for effective management of chronic wounds. Int J Biol Macromol. 2019;132:97–108. https://doi.org/10.1016/j.ijbiomac.2019.03.186

9. Kokabi M, Sirousazar M, Hassan ZM. PVA–clay nanocomposite hydrogels for wound dressing. Eur Polym J. 2007;43(3):773–81. https://doi.org/10.1016/j.eurpolymj.2006.11.030

10. Choi JS, Yoo HS. Pluronic/chitosan hydrogels containing epidermal growth factor with wound-adhesive and photo-crosslinkable properties. J Biomed Mater Res A. 2010;95A(2):564–73. https://doi.org/10.1002/jbm.a.32848

11. Howling GI, Dettmar PW, Goddard PA, Hampson FC, Dornish M, Wood EJ. The effect of chitin and chitosan on the proliferation of human skin fibroblasts and keratinocytes in vitro. Biomaterials. 2001;22(22):2959–66. https://doi.org/10.1016/S0142-9612(01)00042-4

12. Dragostin OM, Samal SK, Dash M, Lupascu F, Pânzariu A, Tuchilus C, Ghetu N, Danciu M, Dubruel P, Pieptu D, Vasile C, Tatia R, Profire L. New antimicrobial chitosan derivatives for wound dressing applications. Carbohydr Polym. 2016;141:28–40. https://doi.org/10.1016/j.carbpol.2015.12.078

13. Gyles DA, Castro LD, Silva JOC, Ribeiro-Costa RM. A review of the designs and prominent biomedical advances of natural and synthetic hydrogel formulations. Eur Polym J. 2017;88:373–92. https://doi.org/10.1016/j.eurpolymj.2017.01.027

14. Iacob A-T, Drăgan M, Ghețu N, Pieptu D, Vasile C, Buron F, Routier S, Giusca SE, Caruntu I-D, Profire L. Preparation, characterization and wound healing effects of new membranes based on chitosan, hyaluronic acid and arginine derivatives. Polymers. 2018;10(6):607. https://doi.org/10.3390/polym10060607

15. Verma J, Kanoujia J, Parashar P, Tripathi CB, Saraf SA. Wound healing applications of sericin/chitosan capped silver nanoparticle incorporated hydrogel. Drug Deliv Transl Res. 2017;7:77–88. https://doi.org/10.1007/s13346-016-0322-y

16. Wang T, Zhu X-K, Xue X-T, Wu D-Y. Hydrogel sheets of chitosan, honey and gelatin as burn wound dressings. Carbohydr Polym. 2012;88(1):75–83. https://doi.org/10.1016/j.carbpol.2011.11.069

17. Xie Y, Liao X, Zhang J, Yang F, Fan Z. Novel chitosan hydrogels reinforced by silver nanoparticles with ultrahigh mechanical and high antibacterial properties for accelerating wound healing. Int J Biol Macromol. 2018;119:402–12. https://doi.org/10.1016/j.ijbiomac.2018.07.060

18. Huang Y, Shi F, Wang L, Yang Y, Khan BM, Cheong K-L, Liu Y. Preparation and evaluation of Bletilla striata polysaccharide/carboxymethyl chitosan/Carbomer 940 hydrogel for wound healing. Int J Biol Macromol. 2019;132:729–37. https://doi.org/10.1016/j.ijbiomac.2019.03.157

19. Kurniasih M. Purwati, Cahyati T, Dewi RS. Carboxymethyl chitosan as an antifungal agent on gauze. Int J Biol Macromol. 2018;119:166–71. https://doi.org/10.1016/j.ijbiomac.2018.07.038

20. Anisha BS, Biswas R, Chennazhi KP, Jayakumar R. Chitosan–hyaluronic acid/nano silver composite sponges for drug resistant bacteria infected diabetic wounds. Int J Biol Macromol. 2013;62:310–20. https://doi.org/10.1016/j.ijbiomac.2013.09.011

21. Sun L, Han J, Liu Z, Wei S, Su X, Zhang G. The facile fabrication of wound compatible anti-microbial nanoparticles encapsulated Collagenous Chitosan matrices for effective inhibition of poly-microbial infections and wound repairing in burn injury care: Exhaustive in vivo evaluations. J Photoch Photobio B. 2019;197:111539. https://doi.org/10.1016/j.jphotobiol.2019.111539

22. Stensberg MC, Wei Q, McLamore ES, Porterfield DM, Wei A, Sepúlveda MS. Toxicological studies on silver nanoparticles: challenges and opportunities in assessment, monitoring and imaging. Nanomedicine. 2011;6(5):879–98. https://doi.org/10.1016/j.jphotobiol.2019.111539

23. Abdel-Mohsen AM, Jancar J, Abdel-Rahman RM, Vojtek L, Hyršl P, Dušková M, Nejezchlebová H. A novel *in situ* silver/hyaluronan bio-nanocomposite fabrics for wound and chronic ulcer dressing: *In vitro* and *in vivo* evaluations. Int J Pharm. 2017;520(1–2):241–53. https://doi.org/10.1016/j.ijpharm.2017.02.003

24. Shi G, Chen W, Zhang Y, Dai X, Zhang X, Wu Z. An Antifouling Hydrogel Containing Silver Nanoparticles for Modulating the Therapeutic Immune Response in Chronic Wound Healing. Langmuir. 2019;35(5):1837–45. https://doi.org/10.1021/acs.langmuir.8b01834

25. Tamer TM, Valachová K, Hassan MA, Omer AM, El-Shafeey M, Eldin MSM, Šoltés L. Chitosan/hyaluronan/edaravone membranes for anti-inflammatory wound dressing: *in vitro* and *in vivo* evaluation studies. Mater Sci Eng C. 2018;90:227–35. https://doi.org/10.1016/j.msec.2018.04.053

26. Berce C, Muresan M-S, Soritau O, Petrushev B, Tefas L, Rigo I, Ungureanu G, Catoi C, Irimie A, Tomuleasa C. Cutaneous wound healing using polymeric surgical dressings based on chitosan, sodium hyaluronate and resveratrol. A preclinical experimental study. Colloids Surf B Biointerafaces. 2018;163:155–66. https://doi.org/10.1016/j.colsurfb.2017.12.041

27. Dehkordi NK, Minaiyan M, Talebi A, Akbari V, Taheri A. Nanocrystalline cellulose–hyaluronic acid composite enriched with GM-CSF loaded chitosan nanoparticles for enhanced wound healing. Biomed Mater. 2019;14(3):035003. https://doi.org/10.1088/1748-605X/ab026c

28. Liu XF, Guan YL, Yang DZ, Yao KD. Antibacterial action of chitosan and carboxymethylated chitosan. J Appl Polym Sci. 2000;79(7):1324–35. https://doi.org/10.1002/1097-4628(20010214)79:7%3C1324::AID-APP210%3E3.0.CO;2-L

29. Bukzem AL, Signini R, Santos DM, Lião LM, Ascheri DPR. Optimization of carboxymethyl chitosan synthesis using response surface methodology and desirability function. Int J Biol Macromol. 2016;85:615–24. https://doi.org/10.1016/j.ijbiomac.2016.01.017

30. Abreu FR, Campana-Filho SP. Preparation and characterization of carboxymethylchitosan. Polímeros. 2005;15(2):79–83. https://doi.org/10.1590/S0104-14282005000200004

31. Gonçalves RC, Silva DP, Signini R, Naves PLF. Inhibition of bacterial biofilms by carboxymethyl chitosan combined with silver, zinc and copper salts. Int J Biol Macromol. 2017;105(Part 1):385–92. https://doi.org/10.1016/j.ijbiomac.2017.07.048

32. Moraes JM, Mendonça DEO, Moura VBL, Oliveira MAP, Afonso CL, Vinaud MC, Bachion MM, Lino Junior RS. Anti-inflammatory effect of low-intensity laser on the healing of third-degree burn wounds in rats. Laser Med Sci. 2012;28:1169–76. https://doi.org/10.1007/s10103-012-1213-1

33. Ribeiro MP, Morgado PI, Miguel SP, Coutinho P, Correia IJ. Dextran-based hydrogel containing chitosan microparticles loaded with growth factors to be used in wound healing. Mater Sci Eng C. 2013;33(5):2958–66. https://doi.org/10.1016/j.msec.2013.03.025

34. Lamaro-Cardoso A, Bachion MM, Morais JM, Fantinati MS, Milhomem AC, Almeida VL, Vinaud MC, Lino-Júnior RS. Photobiomodulation associated to cellular therapy improve wound healing of experimental full thickness burn wounds in rats. J Photochem Photobiol B. 2019;194:174–82. https://doi.org/10.1016/j.jphotobiol.2019.04.003

35. Upadhyaya L, Singh J, Agarwal V, Tewari RP. Biomedical applications of carboxymethyl chitosans. Carbohydr Polym. 2013;91(1):452–66. https://doi.org/10.1016/j.carbpol.2012.07.076

36. Mourya VK, Inamdara NN, Tiwari A. Carboxymethyl Chitosan and its Applications. Adv Mater Lett. 2010;1(1):11–33. https://doi.org/10.5185/amlett.2010.3108

37. Jimtaisong A, Saewan N. Utilization of carboxymethyl chitosan in cosmetics. Int J Cosmet Sci. 2013;36(1):12–21. https://doi.org/10.1111/ics.12102

38. Chen Z, Han L, Liu C, Du Y, Hu X, Du G, Shan C, Yang K, Wang C, Li M, Li F, Tian F. A rapid hemostatic sponge based on large, mesoporous silica nanoparticles and *N*-alkylated chitosan. Nanoscale. 2018;10:20234–45. https://doi.org/10.1039/C8NR07865C

39. Abreu FR, Campana-Filho SP. Characteristics and properties of carboxymethylchitosan. Carbohydr Polym. 2009;75(2):214–21. https://doi.org/10.3390/ijms20235889

40. Matica MA, Aachmann FL, Tøndervik A, Sletta H, Ostafe V. Chitosan as a wound dressing starting material: antimicrobial properties and mode of action. Int J Mol Sci. 2019;20(23):5889. https://doi.org/10.3390/ijms20235889

41. Lee SM, Park IK, Kim YS, Kim HJ, Moon H, Mueller S, Jeong Y-I. Physical, morphological, and wound healing properties of a polyurethane foam-film dressing. Biomater Res. 2016;20:15. https://doi.org/10.1186/s40824-016-0063-5

42. Pawlak A, Mucha M. Thermogravimetric and FTIR studies of chitosan blends. Thermochim Acta. 2003;396(1–2):153–66. https://doi.org/10.1016/S0040-6031(02)00523-3

43. Zawadzki J, Kaczmarek H. Thermal treatment of chitosan in various conditions. Carbohydr Polym. 2010;80(2):394–400. https://doi.org/10.1016/j.carbpol.2009.11.037

44. Rowan MP, Cancio LC, Elster EA, Burmeister DM, Rose LF, Natesan S, Chan RK, Christy RJ, Chung KK. Burn wound healing and treatment: review and advancements. Crit Care. 2015;19:243. https://doi.org/10.1186/s13054-015-0961-2

45. Meuleneire F. An observational study of the use of a soft silicone silver dressing on a variety of wound types. J Wound Care. 2008;17(12):535-9. https://doi.org/10.12968/jowc.2008.17.12.31767

46. Chen X-G, Wang Z, Liu W-S, Park H-J. The effect of carboxymethyl-chitosan on proliferation and collagen secretion of normal and keloid skin fibroblasts. Biomaterials. 2002;23(23):4609–14. https://doi.org/10.1016/S0142-9612(02)00207-7

47. Zhu X, Chian KS, Chan-Park MBE, Lee ST. Effect of argon-plasma treatment on proliferation of human-skin-derived fibroblast on chitosan membrane in vitro. J Biomed Mater Res A. 2005;73(3):264–74. https://doi.org/10.1002/jbm.a.30211

48. Shi C, Zhu Y, Ran X, Wang M, Su Y, Cheng T. Therapeutic Potential of Chitosan and Its Derivatives in Regenerative Medicine. J Surg Res. 2006;133(2):185–92. https://doi.org/10.1016/j.jss.2005.12.013

49. Park CJ, Clark SG, Lichtensteiger CA, Jamison RD, Johnson AJW. Accelerated wound closure of pressure ulcers in aged mice by chitosan scaffolds with and without bFGF. Acta Biomater. 2009;5(6)1926–36. https://doi.org/10.1016/j.actbio.2009.03.002

50. Dhivya S, Padma VV, Santhini E. Wound dressings – a review. Biomedicine. 2015;5(4):24–28. https://doi.org/10.7603/s40681-015-0022-9

51. Strecker-McGraw MK, Jones TR, Baer DG Soft Tissue Wounds and Principles of Healing. Emerg Med Clin North Am. 2007;25(1):1–22. https://doi.org/10.1016/j.emc.2006.12.002

52. Ueno H, Yamada H, Tanaka I, Kaba N, Matsuura M, Okumura M, Kadosawa T, Fujinaga T. Accelerating effects of chitosan for healing at early phase of experimental open wound in dogs. Biomaterials. 1999;20(15):1407–14. https://doi.org/10.1016/S0142-9612(99)00046-0

53. Alsarra IA. Chitosan topical gel formulation in the management of burn wounds. Int J Biol Macromol. 2009;45(1):16–21. https://doi.org/10.1016/j.ijbiomac.2009.03.010

54. Dai T, Tanaka M, Huang Y-Y, Hamblin MR. Chitosan preparations for wounds and burns: antimicrobial and wound-healing effects. Expert Rev Anti Infect Ther. 2011;9(7):857–79. https://doi.org/10.1586/eri.11.59

55. Voigt J, Driver VR. Hyaluronic acid derivatives and their healing effect on burns, epithelial surgical wounds, and chronic wounds: A systematic review and meta-analysis of randomized controlled trials. Wound Repair Regen. 2012;20(3):317–31. https://doi.org/10.1111/j.1524-475X.2012.00777.x

56. Longinotti C. The use of hyaluronic acid based dressings to treat burns: a review. Burns Trauma. 2014;2(4):162-8. https://doi.org/10.4103/2321-3868.142398

57. Mogoşanu GD, Grumezescu AM. Natural and synthetic polymers for wounds and burns dressing. Int J Pharm. 2014;463(2):127–36. https://doi.org/10.1016/j.ijpharm.2013.12.015

58. Mohandas A, Anisha BS, Chennazhi KP, Jayakumar R. Chitosan-hyaluronic acid/VEGF loaded fibrin nanoparticles composite sponges for enhancing angiogenesis in wounds. Colloid Surface B Biointerfaces. 2015;127:105–13. https://doi.org/10.1016/j.colsurfb.2015.01.024

59. Hussain Z, Thu HE, Katas H, Bukhari SNA. Hyaluronic Acid-Based Biomaterials: A Versatile and Smart Approach to Tissue Regeneration and Treating Traumatic, Surgical, and Chronic Wounds. Polymer Rev. 2017;57(4):594–630. https://doi.org/10.1080/15583724.2017.1315433

60. Sanad RA-B, Abdel-Bar HM. Chitosan-hyaluronic acid composite sponge scaffold enriched with Andrographolide-loaded lipid nanoparticles for enhanced wound healing. Carbohydr Polym. 2017;173:441–50. https://doi.org/10.1016/j.carbpol.2017.05.098

61. Chang J, Liu W, Han B, Peng S, He B, Gu Z. Investigation of the skin repair and healing mechanism of N-carboxymethyl chitosan in second-degree burn wounds. Wound Repair Regen. 2013;21(1):113–21. https://doi.org/10.1111/j.1524-475X.2012.00859.x

62. Kweon D-K, Song S-B, Park Y-Y. Preparation of water-soluble chitosan/heparin complex and its application as wound healing accelerator. Biomaterials. 2003;24(9):1595–601. https://doi.org/10.1016/S0142-9612(02)00566-5

63. Liang M, Chen Z, Wang F, Liu L, Wei R, Zhang M. Preparation of self-regulating/anti-adhesive hydrogels and their ability to promote healing in burn wounds. J Biomed Mater Res Part B Appl Biomater. 2019;107(5):1471–82. https://doi.org/10.1002/jbm.b.34239

64. Murakami K, Aoki H, Nakamura S, Nakamura S-I, Takikawa M, Hanzawa M, Kishimoto S, Hattori H, Tanaka Y, Kiyosawa T, Sato Y, Ishihara M. Hydrogel blends of chitin/chitosan, fucoidan and alginate as healing-impaired wound dressings. Biomaterials. 2010;31(1):83–90. https://doi.org/10.1016/j.biomaterials.2009.09.031